11th World Congress on Computational Mechanics (WCCM XI)
5th European Conference on Computational Mechanics (ECCM V)
6th European Conference on Computational Fluid Dynamics (ECFD VI)
July 20 - 25, 2014, Barcelona, Spain

Modelling of Thermoplastic PolyOlefin (TPO) sheets for thermoforming applications

Z. OUESLATI [1]*, M. RACHIK [2]* and M.F. LACRAMPE†

* Université de Technologie de Compiègne, Laboratoire Roberval Centre de Recherches de Royallieu CS 60319 60203 Compiègne Cedex France.
[1]zied.oueslati@utc.fr, [2]mohamed.rachik@utc.fr

† Ecole des Mines de Douai, Dep. Of Polymers and Composites Technology & Mechanical Engineering, 941 rue Ch.Bourseul, Université de Lille Nord de France –F– 59508 Douai, France.
marie-France.Lacrampe@mines-douai.fr

Key Words: *Thermoplastic materials, Constitutive Modelling, Hyperelasticity, Inverse Identification, User Subroutines, Thermoforming.*

Abstract. Thermoplastic PolyOlefin (TPO) materials have proven to be of great interest to automotive applications. The mechanical characteristics of these materials can help to implement solutions to respond to environmental and economical regulatory constraints of the last decade. In fact, beyond their low cost and high degree of recyclability, they allow important light weighting, excellent design flexibility, and high quality whether in terms of visual, tactile and olfactory perceptions. The aim of this study is to model the behaviour of new TPO sheets for thermoforming applications. The studied material can reach very high stretch ranges (up to 800%) and is found to be transversely isotropic. In order to properly predict the thickness distribution of the final thermoformed parts, uniaxial tensile tests were performed along the longitudinal, transverse and diagonal directions, at 5 different temperatures from room temperature to 120°C. A new transversely isotropic hyperelastic model is developed using User Subroutines in Abaqus software. The material parameters at each temperature have been identified using inverse methods, and good results have been obtained. The identification procedure has shown to be difficult because of the high sensitivity of the material parameters and the instability problems at high stretch ranges. This paper focuses on the fitting of the material parameters using the new anisotropic hyperelastic model which have proved to be very flexible and efficient to model different hyperelastic response shapes. On the other hand, the contribution of each material parameter and its effects on the mechanical behaviour has been studied for a faster and a more stable result of the fitting procedure.

1 INTRODUCTION

Several economic and environmental constraints led the automotive industry to develop new materials and new manufacturing processes. The final parts must meet both the high

quality and the low cost requirement. To satisfy these antinomic requirements, new materials like Thermoplastic PolyOlefin sheets were developed and their mechanical properties improved. Generally combined to Polypropylene foams to form a multilayered material that offers a good compromise between several objectives like low cost and high quality. On the other hand, these materials has shown to be adequate for thermoforming applications given that very high stretch ranges can be reached (up to 800 %) and a good thickness repartition of the final part is obtained. In addition, TPO materials offer an important weight gain compared to other materials. All these characteristics led the automotive industry to adopt these materials to manufacture cockpits and door panels for medium and premium car segment. These materials also gave automakers strong commercial and environmental arguments as the colour customization possibilities and the very good recyclability, two highly growing requirements and purchase incentives since years.

When modelling thermoforming applications, hyperelastic constitutive laws are the most adequate to predict the final thickness distribution. This thickness distribution is generally regarded as an important quality criterion of thermoformed parts. . Based on the response shape, the stretch ranges and the experimental data, one must accurately choose one of the several existing hypereleastic models [1,4]. Furthermore, in our case, the sheet manufacturing process of the material induces a noticeable anisotropy which cannot be taken into account with classical existing hyperelastic models. This anisotropic hyperelastic problem is often addressed in biomechanical applications when it comes to soft tissues modelling, and reinforced composites materials. Thus, several anisotropic hyperelastic models have been developed [5,8], to deal with anisotropy problems. The particular case of transverse isotropy is more often used when dealing with calendered plastic sheets. In fact, the growing use of fibrous reinforced materials led authors to develop new transversely hyperelastic models.

In our previous works [9], we used a pseudo fibers approach, to model the incompressible transversely anisotropic hyperelastic behavior of a TPO material with a simple model and we faced some instability and accuracy problems during calculations. We concluded that the most efficient way is to decompose the energy potential into an isotropic part and an anisotropic part which represent the pseudo fibers contribution. The Material is then considered as an isotropic hyperelastic matrix and a transversely isotropic reinforcement. The method is very efficient and allows to properly predicting the material behavior in several fibers orientations, only if the material parameters are accurately identified.

In this work, material parameter identification at several temperature and orientation is focused on. A new simple transversely isotropic hyperelastic model is used and the results are very convincing whether in terms of accuracy or stability. In the second section, isotropic and transversely isotropic hyperelasticity constitutive equations are presented. In section 3 the used model is briefly described. Finally, the experimental data and the identification results are presented.

2 CONSTITUTIVE EQUATIONS FOR HYPERELASTICITY

4.1 Isotropic hyperelasticity

Hyperelastic behaviour is described in terms of a strain energy density potential W, which must satisfy some trivial conditions like the objectivity and the state free conditions. W can be written as a function of principal stretches or in terms of the strain invariants. Let x be the

current position e.g. the spatial coordinates and X the reference position e.g. the material coordinates of the same particle. The deformation gradient tensor F is defined by:

$$F = \frac{\partial x}{\partial X} \tag{1}$$

The total volume change J is found to be:

$$J = \det(F) \tag{2}$$

To handle the incompressibility in a straightforward manner, we need to define the isochoric deformation gradient tensor $\bar{F}$ as:

$$\bar{F} = J^{-\frac{1}{3}}.F \tag{3}$$

As Abaqus user subroutines require the Cauchy stress, the appropriated strain measure for the formulation of the constitutive model is the left Cauchy stress tensor B is used. The isochoric part of B is defined by:

$$\bar{B} = \bar{F}.\bar{F}^{T} \tag{4}$$

The invariants of the left Cauchy-Green strain tensor and their relations to the principal stretches are recalled hereafter:

$$\begin{cases} \bar{I}_1 = tr(\bar{B}) \\ \bar{I}_2 = \frac{1}{2}\left[tr(\bar{B})^2 - tr(\bar{B}^2) \right] \\ \bar{I}_3 = \det(\bar{B}) \end{cases} \tag{5}$$

And

$$\begin{cases} \bar{I}_1 = \bar{\lambda}_1 + \bar{\lambda}_2 + \bar{\lambda}_3 \\ \bar{I}_2 = \bar{\lambda}_2.\bar{\lambda}_3 + \bar{\lambda}_3.\bar{\lambda}_1 + \bar{\lambda}_1.\bar{\lambda}_2 \\ \bar{I}_3 = \bar{\lambda}_1.\bar{\lambda}_2.\bar{\lambda}_3 \end{cases} \tag{6}$$

For an isotropic compressible material, the strain energy potential W can be written as function of the strain invariants $\bar{I}_i$ or the principal stretches $\bar{\lambda}_i$ and J .For commodity sake, it is split into an isochoric part $\bar{W}$ and a volumetric part :

$$W(\bar{I}_i, J) = \bar{W}(\bar{I}_i) + U(J) = \bar{W}(\bar{\lambda}_i) + U(J) \tag{7}$$

The Cauchy stress is decomposed into the deviatoric stress s and the equivalent pressure p as:

$$\sigma = s - p\,\mathrm{I} \tag{8}$$

I is the unit second order tensor. The deviatoric part of σ is derived from the isochoric part of the strain energy potential while the equivalent pressure is derived from the volumetric part:

$$s = \frac{2}{J} dev(\bar{B}\frac{\partial W}{\partial \bar{B}}) \qquad (9)$$
$$p = -\frac{\partial U}{\partial J}$$

In this paper and as in our previous work, a third order Ogden model is used. For a compressible material, The Ogden strain energy function is expressed in terms of the principal stretches $\bar{\lambda}_i$ and J:

$$W(\bar{\lambda}_1, \bar{\lambda}_2, \bar{\lambda}_3, J) = \sum_{i=1}^{N} \frac{2\mu_i}{\alpha_i^2}\left[\bar{\lambda}_1^{\alpha_i} + \bar{\lambda}_2^{\alpha_i} + \bar{\lambda}_3^{\alpha_i} - 3\right] + \sum_i \frac{1}{D_i}(J-1)^{2i} \qquad (10)$$

μ_i , α_i and D_i are material parameters.

From Eq.9 and Eq.10, the principal deviatoric stresses s_i and the equivalent pressure p are given by:

$$s_i = \frac{2}{J} dev(\sum_{i=1}^{N} \frac{\mu_i}{\alpha_i} \bar{\lambda}_i^{\alpha_i}) \qquad (11)$$
$$p = \sum_i \frac{2i}{D_i}(J-1)^{2i-1}$$

As the main application of this work, is the thermoforming simulation of thin plastic sheet, the plane stress assumption is considered. In addition, the material is supposed to be incompressible. In this case, *J=1, U(J)=0* and the equivalent pressure can be computed with the help of the plane stress assumption:

$$\sigma_3 = s_3 - p = 0 \Rightarrow p = \sum_{i=1}^{N} \frac{2\mu_i}{\alpha_i} \bar{\lambda}_3^{\alpha_i} = \sum_{i=1}^{N} \frac{2\mu_i}{\alpha_i} \bar{\lambda}_1 \bar{\lambda}_2^{-\alpha_i} \qquad (12)$$

4.2 Transversely Isotropic hyperelasticity

The calendered plastic sheets exhibit a preferred direction and the material responses in the longitudinal and the transverse directions can be significantly different. Thus it is important to take into account this anisotropy as it can affect the quality of the final parts. The anisotropic hyperelastic behavior has been focused on during the last decades due to the great advances in biomechanical engineering and reinforced materials [10,12]. Several models have been developed using different physical or mathematical approaches [13, 17]. For our work, the pseudo fibers approach which consists in considering the material as a combination of an isotropic hyperelastic matrix and a transversely isotropic fibers contribution is the most appropriated. The isochoric part of the deformation energy potential is decomposed into an isotropic contributions $\bar{W}_{iso}$ and a transversely anisotropic contribution $\bar{W}_{trsv}$:

$$\bar{W} = \bar{W}_{iso} + \bar{W}_{trsv} \qquad (13)$$

The transversely isotropic part of the strain energy potential must meet some elementary requirement of material frame invariance. To outline these requirements, let a_0 to be the unit

directional vector of the pseudo-fibers. The orientation tensor A is defined in our case as:

$$A = a_0 \otimes a_0 \tag{14}$$

$\bar{W}_{trsv}$ should satisfy the following equation or any orthogonal transformations Q.

$$\bar{W}(\bar{B}) = \bar{W}(\bar{B}, A) = \bar{W}(Q\bar{B}Q^T, QAQ^T) \tag{15}$$

Consequently, $\bar{W}_{trsv}$ should be a function of following pseudo-invariants:

$$\begin{cases} I_4 = tr(\bar{B} : A) \\ I_5 = tr(\bar{B}^2 : A) \\ I_6 = tr(\bar{B} : A^2) \\ I_7 = tr(\bar{B}^2 : A^2) \end{cases} \tag{16}$$

To meet the material symmetries requirements, only the I_4 pseudo invariant representing one family of pseudo fibers is used $\bar{W}_{trsv}$ can then be expressed as:

$$\bar{W}_{trsv} = \bar{W}_{trsv}(I_4) \tag{17}$$

From Eq.8, the pseudo fiber contribution to the deviatoric stress can be expressed as*:*

$$s_{trsv} = \frac{2}{J} dev(\bar{B} \frac{\partial \bar{W}_{trsv}}{\partial I_4} \frac{\partial I_4}{\partial \bar{B}}) \tag{18}$$

Where

$$\frac{\partial I_4}{\partial \bar{B}} = a_0 \otimes a_0 \tag{19}$$

3 FINITE ELEMENT AND EXPERIMENTAL VALIDATIONS

In several works [18,21], only one material parameter is often adequate to properly model the fibers contribution and to predict the material behavior in different orientations. Using the same forms in our case led to several instability and lake of accuracy. To remedy these problems, we suggested multiparameter models in our previous works. Thus, the proposed model is an extension of a third order Ogden model and three C_i parameters are used to model the transversely isotropic part. The strain energy potential is written as follow:

$$\bar{W}(\bar{\lambda}_1, \bar{\lambda}_2, \bar{\lambda}_3, I_4) = \sum_{i=1}^{3} \frac{2\mu_i}{\alpha_i^2} \left[\bar{\lambda}_1^{\alpha_i} + \bar{\lambda}_2^{\alpha_i} + \bar{\lambda}_3^{\alpha_i} - 3 \right] + \sum_{p=1}^{3} C_p . (I_4 - 1)^p \tag{20}$$

The material parameters are fitted to measurements data at different temperatures. The tensile tests are performed in the longitudinal, transverse and diagonal directions, respectively referred to in this paper as the 0°, 90° and 45° directions. On the other hand, considering the material behavior and the adopted energy form of the pseudo fibers contribution, the following fitting procedure is used:

i. The parameters of the isotropic part μ_i and α_i, *i=1...3*, are fitted the data from the 90°

direction test.

ii. The parameters of the transversely isotropic part C_i are calibrated on the data from to the 0° direction test.

iii. The data from the 45° direction test is finally predicted and the identified parameters are checked.

The Ogden model was successfully implemented in Abaqus software using Vumat user subroutines as shown in Fig.1.

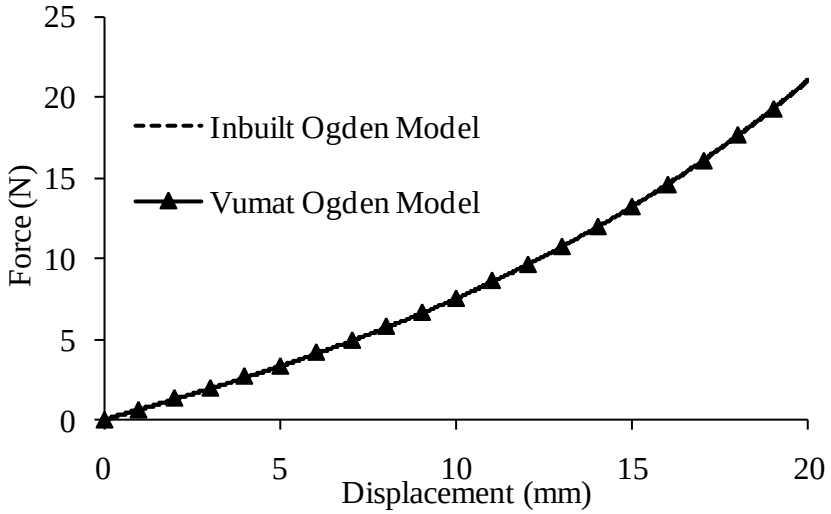

Figure 1: Comparison between the predictions from the user material and those obtained with Abaqus.

Besides, the tensile test specimen has a rectangular shape (*L=20mm, l=15mm, e=0.56mm*) and is modeled using a *5x5* quadratic 2D solid elements as shown in Fig.2.

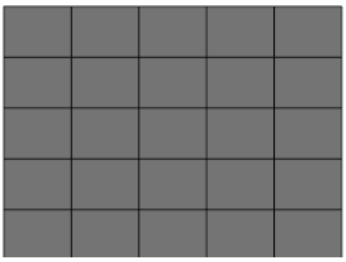

Figure 2: Mesh and specimen geometry

The results of the material constants fitting to experimental data at the 45°C, 70°C, 90°C and 120°C temperatures are illustrated in Fig.3 to Fig.5. It's worth noting the very high stretch ranges that were reached during the hot tensile tests (up to 700% at 120°C).Although, good results are obtained and the use of an Ogden model is justified. In fact, unlike other well known models (Mooney-Rivlin, Neo Hook, Yeoh…etc) the Ogden model offers a high flexibility concerning the response shape on one hand, and provides a higher stability especially when incompressibility condition is taken into account on the other.

The identification of the isotropic part parameters shows very good agreement with the

experimental data. A small error is noticeable at the beginning of the deformation (*10 mm* of the total displacement) at the different temperatures. Yet the identification results are good enough.

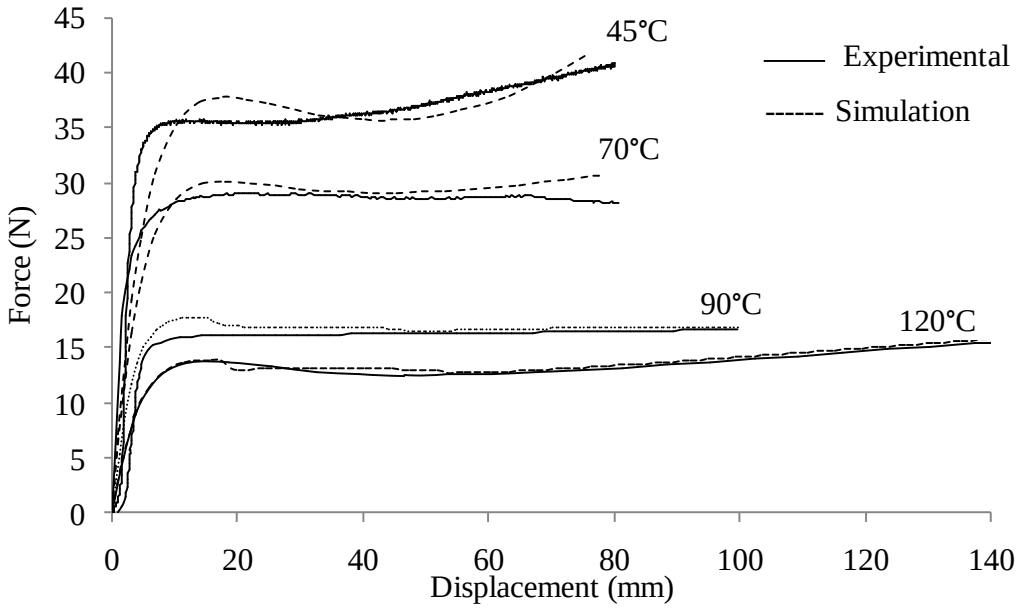

Figure 3: Comparison between the predictions from the best fit of μ_i and α_i and the measurements from the 90° direction test

The results of the calibration of the transversely isotropic parameters according to the 0° orientation are illustrated in Fig.4.

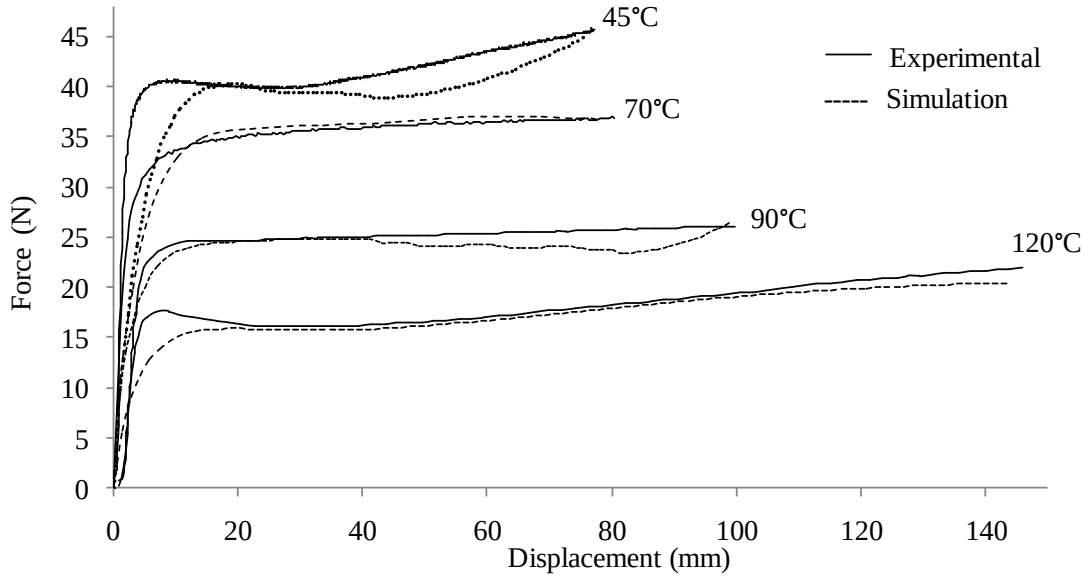

Figure 4: Comparison between the predictions from the best fit of C_i and the measurements from the 0° direction test

In a general, good results are obtained at the different temperatures even at very high stretch ranges. The same error is observed at the beginning of the deformation. Finally, the results of the prediction of the 45° orientation are illustrated in Fig.5. The predictions are in good agreement with the measurements.

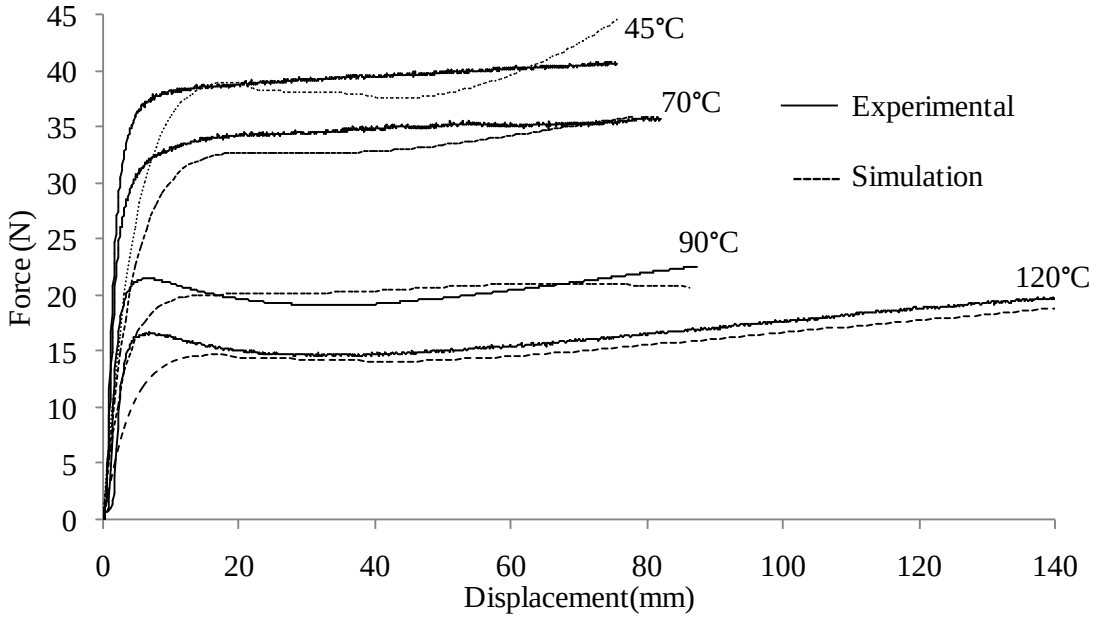

Figure 5: Comparison between the predictions from the best fit of μ_i , α_i and C_i and the measurements from the 45° direction test

Furthermore, to illustrate the consistency of the inverse identification procedure, Fig.6 shows the evolution of the initial Young's modulus with respect to the temperature due to the material softening.

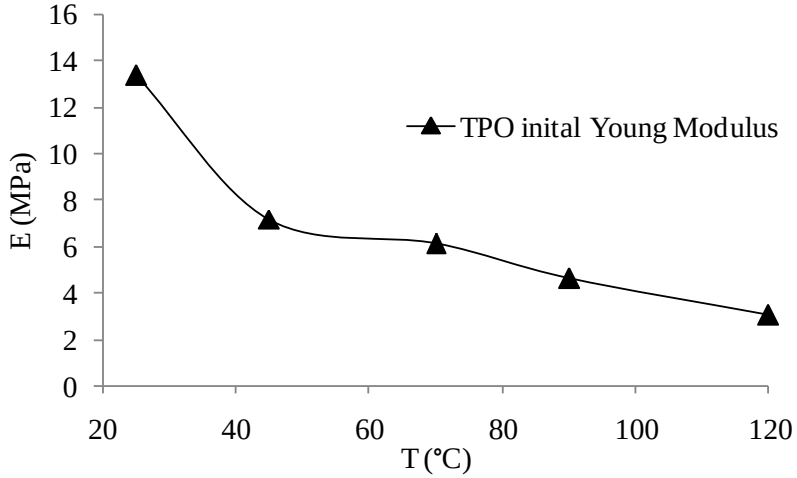

Figure 6: Evolution of the initial Young's modulus with the temperature

Hence, the main conclusion to be drawn from the material constants fitting procedure is the reliability of the proposed model and the convincing final results. Moreover, it is important to note that a very large number of iterations can be reached in some cases, while an accurate result is not assured. For more efficiency, the material parameters were investigated and their effect on the material response shape was studied.

Table.1 illustrates the signs of the material constants when a stable result is reached. When this constraint sign is prescribed, the iterations number decreases remarkably and the stability of the final result is assured.

Table 1: Signs of obtained material parameters

Parameter	α_1	α_2	α_2	μ_1	μ_2	μ_3	C_1	C_2	C_3
Sign	(+)	(+)	(-)	(-)	(+)	(+)	(+)	(-)	(+)

On the other hand,it is interesting to understand the effect of the C_i transversely isotrpic constants on the response shape. In fact, every parameter influences a portion of the reponse and controls the curve shape in that part. Thus, the following observations were verfied and helped to significally decrease the iterations number by avoiding completly random strating parameter sets.

i. $0 < C_1\ (Mpa) < 0.1$ and controls the initial part of the reponse (under *20%* of total the displacement) and influences the initial stiffness value.
ii. $-0.01 < C_2\ (Mpa) < 0$ and controls the region of the reponse (between *20%* and *70%* of the total displacement).
iii. $0 < C_3\ (Mpa) < 10^{-4}$ and controls the final part of the reponse.

Fig.7 illustrates an example of the C_i constants calibration procedure. When the the above constraints are imposed on the starting parameters set at the very first iteration, the C_i constants can be easily calibrated, and the final result is generally very convincing.

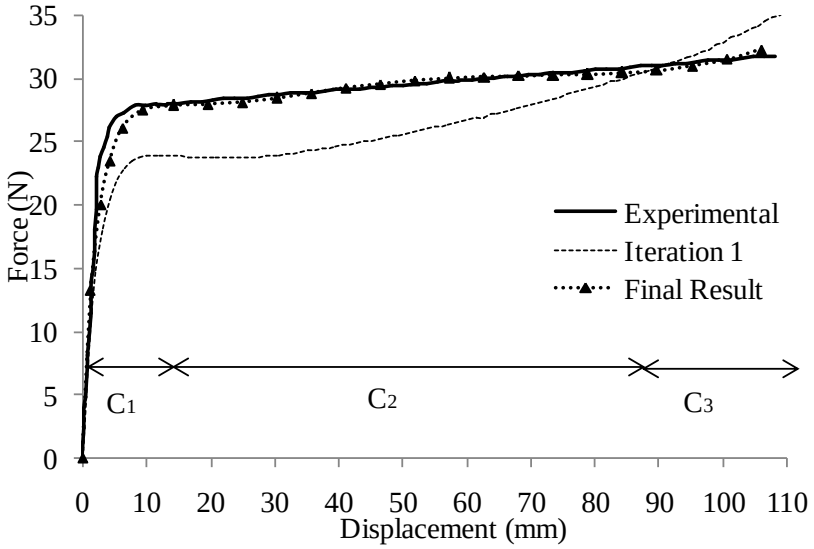

Figure 7: Effects of the C_i parameters on the response shape

Another key finding is the high sesitivity of the material parameters especially the α_i Ogden constants. Thus, to assure an accurate and stable result, it was essential to decrease the incremetations values in order to avoid a divergent calculation as shown in Fig.8.

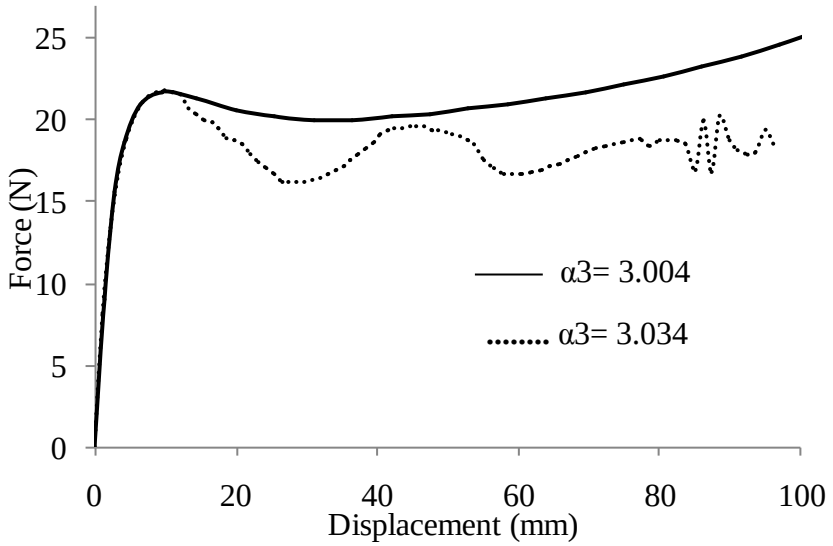

Figure 8: Response shape sensitivity to the α_i parameters

In a general, several difficulties were faced during the inverse identification procedure of the TPO material. Beyond accuracy and stability matters, investigation works have been conducted beforehand in order to reduce the iterations number and to assure a reliable result.

1 CONCLUSION

In this paper, the incompressible transversely isotropic hyperelastic behavior of a TPO material was investigated at different temperatures. A new form of the transversely isotropic strain energy form is proposed and proved to be very efficient whether in terms of accuracy or stability. In addition, we have carried out a study of the fitting of material constants to experimental data. This helped to considerably reduce the number of iterations and to enhance the accuracy of the final result.

Furthermore, numerical considerations have been taken into account to assure the calculations convergence, especially when incompressibility condition is considered.

As a perspective to this work, 3D image correlation techniques will be used to measure displacement fields during a thermoforming process. Thus, higher temperatures can be reached and technical difficulties during hot tensile test can be avoided and the identified parameters reliability can be checked.

REFERENCES

[1] Mooney, M.A. Theory of large elastic deformation. *J. Appl. Phys*(1940)**11**:582-592.

[2] Ogden, R.W. Large deformation isotropic elasticity - on the correlation of theories and experiment for uncompressible rubberlike solids. *Proc. R. Soc. A*(1972)**326**:565-584.

[3] Arruda, E.M. and Boyce, M.C. A three-dimensional constitutive model for the large stretch behaviour of rubber elastic materials. *J. Mech. Phys. Solids*(1993)**42**:389-412.

[4] Yeoh, O.H.Some forms of the strain energy function for rubber. Rubber. *Chem. Techno*(1993)**66**: 754-771.

[5] Chuong. C.J. and Fung, Y.C. Three-dimensional stress distribution in arteries. ASME *J. Biomech. Eng*(1983)**105**:268–274.

[6] Holzapfel, G.A. and Eberlein, R. and Wriggers, P.H. and Weizsacker, W. Large strain analysis of soft biological membranes: formulation and finite element analysis. *Comput. Method. Appl. M*(1996)**132**:45–61.

[7] Holzapfel, G.A. and Gasser, T.C. and Ogden, R.W. A new constitutive framework for arterial wall mechanics and comparative study of material models. *J. Elasticity*(2000)**61**: 1-48.

[8] Peng, X.Q. and Guo, Z.Y. and Moran, B. An Anisotropic Hyperelastic Constitutive Model with Fiber-Matrix Shear Interaction for the Human Annulus Fibrous. *J. Appl. M*(2006)**73**: 815-824.

[9] Oueslati, Z. and Rachik, M. and Lacrampe, M.F. Transversely isotropic hypereleastic constitutive models for plastic thermoforming simulation. *Key Engineering Material.* (2013)**554-557**:1715-1728.

[10] Aimene, Y. and Hagege, B. Sidoroff, F. and Salle, E. and Boisse, P. Hyperelastic approch for composite reinforcing forming simulations. ESAFORM 2008. *Int. J. Mat. Form*(2008)**1**:811-814.

[11] Vidal-Sallé, E. and Aimène, Y. Boisse, P. Use of a hyperelastic constitutive law for dry woven forming simulations. *International Conference on Material Forming*. ESAFORM (2011)**1353**:883-888.

[12] Xiongqi, P. and Zaoyang, G. and Tongliang D. and Woong-Ryeol, Y. A simple anisotropic hyperelastic constitutive model for textile fabrics with application to forming simulation. *Composites: Part B*(2013)**52**:275–281.

[13] Ball, J.M. Convexity conditions and existence theorems in non linear elasticity. *Arch. Rational. Mech. Anal*(1977)**63**:337-403.

[14] Hartmann, S. and Neff, P. Polyconvexity of generalized polynomial-type hyperelastic strain energy functions for near-incompressibility.*Int. J. Solids. Struct(*2003)**40**:2768-2791.

[15] Schröder, J. and Neff, P. Invariant formulation of hyperelastic transverse isotropy based on polyconvex free energy functions. *Int. J. Solids. Struc*(2003)**40**:401-445.

[16] Itskov, M. A generalized orthotropic hyperelastic material model with application to incompressible shells. *Int J. Numer. Meth. Eng*(2001)**50**:1777-1799.

[17] Itskov, M. and Ehret, A.E. A class of orthotropic and transversely isotropic hyperelastic constitutive models based on a polyconvex strain energy function. *Int. J. Solids. Struct*(2004)**41**:3833–3848.

[18] Erchiqui, F. and Bendada, A. and Gakwaya, A. Analysis of Long Fibers Direction of Transversely Isotropic Hyperelastic Material for Thermoforming Application *J. Reinf. Plast. Compos*(2005)**24**: 961-975.

[19] Chevaugeon, N. and Verron, E. and Peseux, B. Finite element analysis of nonlinear transversely isotropic hyperelastic membranes for thermoforming applications. *European Congress on Computational Methods in Applied Sciences and Engineering* (ECCOMAS), Barcelone(2000).

[20] Weiss, J.A. and Maker, B.N. and Govindjee, S. Finite element implementation of incompressible, transversely isotropic hyperelasticity. *Comput. Method. Appl. M*(1996) **135**:107-128.

[21] Kyriacou, S. K.and Schwab, C. and Humphrey, J. D. Finite element analysis of nonlinear orthotropic hyperelastic membranes. *Comput. Mech*(1996)**18**:269-278.